IN-SILICO SCREENING OF PLANT-DERIVED NATURAL COMPOUNDS FOR THEIR ANTI- COVID-19 POTENTIAL

VANDITA ANAND, SAUMYA SRIVASTAVA AND ANJANA PANDEY *

Department of Biotechnology, Motilal Nehru National Institute of Technology (MNNIT) Allahabad, Prayagraj-211004, India.

ABSTRACT

The novel coronavirus disease 2019 (COVID-19) caused by severe acute respiratory syndrome coronavirus 2 (SARS-CoV-2) began in Wuhan, China, in December 2019 and quickly spread across the worldwide. It becomes a global pandemic and risk to the healthcare system of almost every nation around the world. In this study thirty natural compounds of 19 Indian herbal plants were used to analyze their binding with eight proteins associated with COVID -19. Based on the molecular docking as well as ADMET analysis, isovitexin, glycyrrhizin, sitosterol, and piperine were identified as potential herbal medicine candidates. On comparing the binding affinity with Ivermectin, we have found that the inhibition potentials of the *Trigonella foenum-graecum* (fenugreek), *Glycyrrhiza glabra* (licorice), *Tinospora cordifolia* (giloy) and *Piper nigrum* (black pepper) are very promising with no side-effects.

Keywords: COVID-19, SARS-CoV-2, Indian herbal plants, Natural compounds, Docking, ADMET analysis.

INTRODUCTION

Coronaviruses are a group of viruses belonging to the subfamily Orthocoronavirinae in the family Coronaviridae, order Nidovirales, which infect both animals and humans. A new coronavirus that previously has not been identified in humans emerged in Wuhan, China in December 2019 (1). It causes an unusual type of pneumonia with symptoms, such as fever, cough, muscle soreness, headache, sore throat, chest pain, diarrhea, nausea, and vomiting (2).

Coronaviruses contain spike-like projections of glycoproteins on their surface, which seem like a crown under the electron microscope. The genome of coronavirus encodes structural and non-structural proteins. The structural proteins are responsible for host infection (3), membrane fusion (4), viral assembly (5), morphogenesis, and release of virus particles (6), while the non-structural proteins (nsps) promote viral replication and transcription (7).

The World Health Organization (WHO; https://www.who.int) on 12 January 2020 temporarily designated the virus causing this disease as the 2019 novel coronavirus (2019-nCoV). On 11 February 2020, this infectious disease coronavirus disease (COVID-19) was officially renamed by the WHO. At present, the COVID-19 pandemic is spreading all over the world.

India is a heritage of invaluable herbal plants which used have medical and therapeutic properties. In India herbal plants were used for medicinal purposes even before prehistoric times. There is evidence that for over 4000 years Unani Hakims, Ayurveda, and European and Mediterranean cultures used herbs as medicine (8). The medicines prepared from parts of plant (leaves, flowers, seeds, roots, bark, stems, etc.) are known as herbal drug (9). Herbal plant treatment is considered to be very safe, since there are no or minimal side effects. The extraction and characterization of bioactive compounds from these herbal plants have resulted in the introduction of new drugs with high medicinal value (10). The various ranges of bioactive nutrients present in these natural products play a crucial role in the prevention and cure of different diseases. Plant-derived compounds are secondary metabolites, which play a vital role as antimicrobials and antivirals and are classified in many groups, such as alkaloids, phenolics, flavonoids, terpenes, quinones, saponins, etc. (11). Plant medicinal properties could be based on the antioxidant, antipyretic, antimicrobial effects of the phytochemicals in them. The aspect described made the virtual screening method promising and useful in developing new herbal remedies to satisfy the many clinical needs. Medicinal plants contain bioactive compounds that are primarily used in medicinal applications.

The COVID-19 proteins are involved in binding and promote viral replication and transcription. The SARS-CoV-2 N protein is a binding protein involved in viral RNA replication (12). The SARS-CoV-2 RNA polymerase is a multimeric complex that encompasses the core catalytic domain Nsp12, which has little activity until complexed with the Nsp7 and 8 co-factors (13). Nsp9 is thought to play a similarly essential role in viral RNA replication as a single-stranded RNA binder in SARS-CoV (14). Nsp15 viruses contain a cluster of conserved enzymes as part of their ORF1a/b polyproteins, a Nidoviral RNA uridylate-specific endonuclease (NendoU) is one such protein whose activity degrades polyuridine RNA extensions (15). Nsp3 contains a papain-like protease domain that cleaves polyprotein in SARS-CoV-2 and associated SARS-CoVs to release Nsp1, 2 & 3 (16). Nsp5, also referred to as main protease ($3CL^{pro}$) and main protease (M^{pro}) is a pro-enzyme that auto-processes and releases Nsp4 to Nsp16 (17). Along with the Nsp10/Nsp16 interface, the structures highlight the S-adenosyl-L-methionine and RNA cap substrate binding pockets as opportunistic features for the development of antiviral therapeutics (18). Clathrin-mediated internalization begins with the redistribution of selected transmembrane receptors into a plasma membrane region coated with a polyhedral clathrin lattice on the cytosolic face (19).

This paper reports the results of modelling of molecular docking of COVID-19 proteins with herbal natural compounds to find out their respective binding energies. The virtual screening methods are routinely and extensively used to reduce the cost and time for drug discovery (20). The study was further validated by the use of *in silico* ADMET (Absorption, Distribution, Metabolism, Excretion and Toxicity) assessment of selected natural compounds in order to check their pharmacokinetics and pharmacodynamics properties to predict effective drugs for COVID-19 treatment.

MATERIALS AND METHODS

Proteins

Present work was mainly focused on nine proteins associated with COVID-19. The 3D structures for these proteins was downloaded from PDB (Protein Data Bank) by using URL http://www.rcsb.org/PDB. The names and PDB Id of the retrieved proteins are represented in Table 1. The PDB structure of COVID-19 proteins was prepared by removing all the water molecules and adding hydrogen atoms and Kollman charges. For further studies the proteins files were saved into PDBQT format and finally optimized for docking using AutoDock Tools 1.5.6.

Table 1. The names and PDB Id of the retrieved proteins.

S.No.	PDB Id	Names
1.	6M3M	SARS-CoV-2 nucleocapsid protein N-terminal RNA binding domain (NP)
2.	6M71	RNA-dependent RNA polymerase (NSP12) in complex with cofactors
3.	6VWW	Endoribonuclease from SARS CoV-2 (NSP15)
4.	6W9C	Papain-like protease (NSP3)
5.	6WXD	RNA-replicase (NSP9)
6.	6Y2E	Main Protease (NSP5)
7.	6YHU	nsp7-nsp8 complex of SARS-CoV-2
8.	7C2J	nsp16-nsp10 heterodimer (N7- and 2'O-methyltransferases) in complex with SAM
9.	1UTC	Clathrin terminal domain complexed with TLPWDLWTT

*Corresponding author email: anjanap@mnnit.ac.in

Ligands

Ligands against these proteins were selected from the Indian herbal plants and they were retrieved from PubChem database. The SMILES (Simplified Molecular Input Line Entry Specification) of all the twenty compounds were downloaded from PubChem (https://pubchem.ncbi.nlm.nih.gov/). The names and molecular formulae of the retrieved compounds are represented in (Table 2). The names and molecular formulae of the retrieved drugs are represented in supplementary Table 1. The structure of all compounds were drawn with SMILES and saved in MOL format using Chemsketch software. All compounds were converted from MOL format to PDB format and saved using the Open Babel tool (21). For further studies the ligand files were saved into PDBQT format and finally optimized for docking using AutoDock Tools 1.5.6.

Table 2- The names and molecular formulae of the retrieved compounds.

S.No.	Indian Herbal plants	Natural compounds	Mol. formula
1.	*Syzygium aromaticum* (cloves)	Eugenol	$C_{10}H_{12}O_2$
		Eugenyl acetate	$C_{12}H_{14}O_3$
2.	*Cinnamomum verum* (cinnamon)	Cinnamaldehyde	C_9H_8O
3.	*Allium sativum* (garlic)	Allicin	$C_6H_{10}OS_2$
4.	*Myristica fragrans* (nutmeg)	Catechins	$C_{15}H_{14}O_6$
5.	*Trigonella foenum graecum* (fenugreek)	Rhaponticin	$C_{21}H_{24}O_9$
		Isovitexin	$C_{21}H_{20}O_{10}$
6.	*Bunium bulbocastanum* (black cumin)	Thymoquinone	$C_{10}H_{12}O_2$
7.	*Cinnamomum tamala* (bay leaf)	α -pinene	$C_{10}H_{16}$
8.	*Enicostemma Littorale* (bitter-stick)	Swertiamarin	$C_{16}H_{22}O_{10}$
		Mangiferin	$C_{19}H_{18}O_{11}$
9.	*Glycyrrhiza glabra* (licorice)	Glycyhrrizin	$C_{42}H_{62}O_{16}$
10.	*Tinospora cordifolia* (giloy)	Berberine	$C_{20}H_{18}NO_4^+$
		Sitosterol	$C_{29}H_{50}O$
11.	*Curcuma longa* (turmeric)	Curcumin	$C_{21}H_{20}O_6$
12.	*Zingiber officinale* (ginger)	Gingerol	$C_{17}H_{26}O_4$
		Shogaol	$C_{17}H_{24}O_3$
13.	*Trachyspermum ammi* (ajwain)	Thymol	$C_{10}H_{14}O$
14.	*Piper nigrum* (black pepper)	Piperine	$C_{17}H_{19}NO_3$
15.	*Amomum subulatum* (badi ilaichi)	1,8-cineole	$C_{10}H_{18}O$

Molecular Docking of Protein and Ligand

Molecular docking is considered as the "key and lock" hypothesis used to find the best fit orientation of ligand and protein. Using AutoDock Tools 1.5.6 (22), target proteins were docked with selected natural compounds and binding energy was calculated. The prepared files of the protein and ligands were submitted to AutoDock Tool. During the docking procedure, the various conformations for ligand were generated, but the best conformations with minimal energy was considered as output.

ADME and Toxicity analysis

A reliable ADMET predictive model can be useful for the estimation of physicochemical parameters such as logP and logS. The ALOGPS 2.1 tool (http:/www.vcclab.org/lab/alogps/) (23) was used to conduct the ADME analysis of the selected natural compounds. The molecular structure of compounds was submitted to ADMET-SAR server (http://lmmd.ecust.edu.cn/admetsar1/home/) (24) to examine their different pharmacokinetic and pharmacodynamic parameters including blood brain barrier penetration, carcinogenicity, subcellular localization, LD50 and category of acute oral toxicity.

RESULTS & DISCUSSION

PDB Structures of selected Proteins

The retrieved PDB structure is presented in Fig. 1.

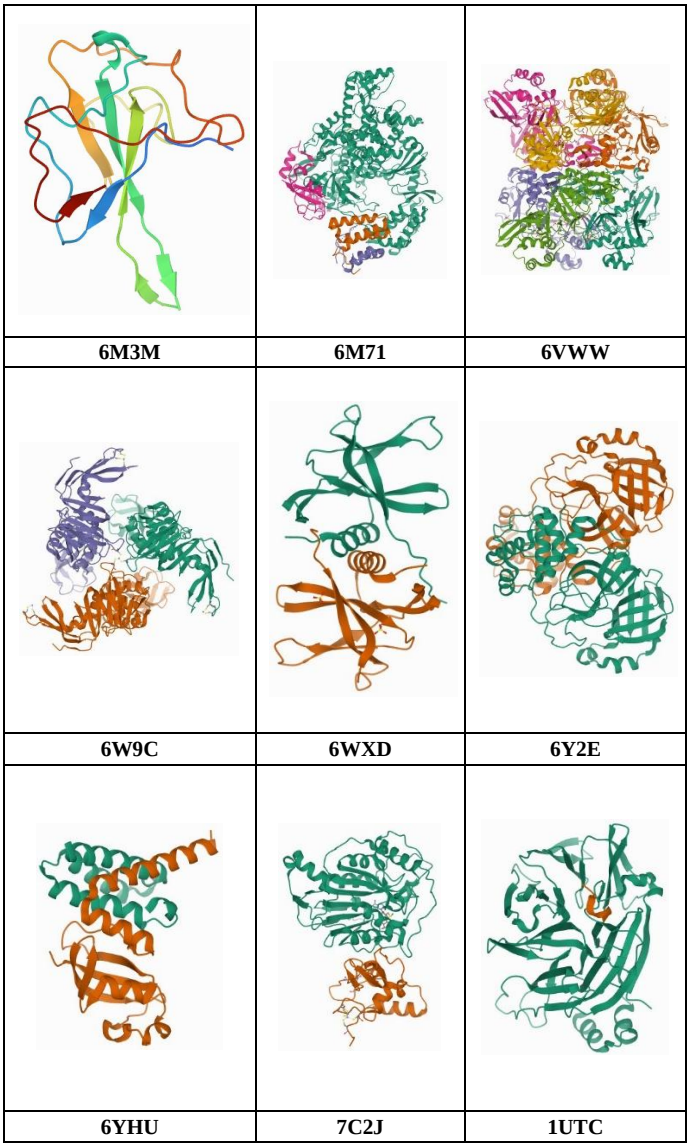

Figure 1. 3-dimensional structures of proteins associated with COVID-19 (see Table 1 for abbreviations).

Docking

Binding of COVID-19 proteins with selected ligands

The virtual screening utilizes docking and scoring of compounds from a dataset and predicts the binding modes and affinities of ligand and protein. The molecular docking studies of the COVID-19 proteins with Indian herbal plant natural compounds were performed using AutoDock Tools 1.5.6. Molecular docking assumes that a compound is absorbed perfectly and interacted with the receptor. The lowest binding energy indicates the most significant interaction between ligand and protein (25). The results of the molecular docking studies along with binding energies are shown in Table 4. Table 3 demonstrates that the ligand 7 (isovitexin) has minimal binding affinity (ΔG) values with papain- like

protease (NSP3) (6W9C) and RNA-replicase (NSP9) (6WXD) are -8.24 and -9.36 kcal/mol. Ligand 12 (glycyrrhizin) has minimal binding affinity (Δ*G*) values at SARS-CoV-2 nucleocapsid protein N-terminal RNA binding domain (NP) (6M3M), nsp7-nsp8 complex of SARS-CoV-2 (6YHU) and nsp16-nsp10 heterodimer (N7- and 2'O-methyltransferases) in complex with SAM (7C2J) are -10.9, -7.93 and -8.58 kcal/mol. Ligand 14, i.e., Sitosterol having minimal binding affinity (Δ*G*) values at RNA-dependent RNA polymerase (NSP12) in complex with cofactors (6M71), Endoribonuclease from SARS CoV-2 (NSP15) (6VWW) and Clathrin terminal domain complexed with TLPWDLWTT (1UTC) are -7.19, -9.32, and -10.03 kcal/mol. Ligand 19, i.e., Piperine having minimal binding affinity (Δ*G*) values at Main Protease (NSP5) (6Y2E) are -7.28 kcal/mol.

The docking images of different ligands with COVID-19 proteins are represented in Fig. 2, where the formed hydrogen bonds are represented by green lines. The lengths of the formed hydrogen bonds was measured. The binding affinity (Δ*G*) of compounds depends on the type of bonding (H-bond) that occurs with the active site of the protein. The results of docking of the ligand 7, 12, 14, 19 (isovitexin, glycyrrhizin, sitosterol, and piperine) with nine proteins associated with COVID-19 are given in a Supplementary Tables 3-7.

Isovitexin formed two hydrogen bond of lengths 2.135 Å and 1.593 Å with the isoleucine (ILE-97) and serine (SER-98) of chain A in endoribonuclease from SARS CoV-2 (NSP15) (6VWW). Similarly, Isovitexin exhibited binding with lysine (LYS-217) and lysine (LYS-306) of chain A of Papain-like protease (NSP3) (6W9C) with hydrogen bond lengths of 1.693 Å and 1.827 Å, while Isovitexin with RNA-replicase (NSP9) (6WXD) formed hydrogen bond of bond lengths 2.049 Å with the serine (SER-59) of chain B.

Glycyrrhizin with SARS-CoV-2 nucleocapsid protein N-terminal RNA binding domain (NP) (6M3M) formed three hydrogen bond of bond lengths 1.869 Å, 2.052 Å and 2.096 Å with the asparagine (ASN-112), lysine (LYS-66) and asparagine (ASN-155) of chain A, B and D, respectively. Similarly, Glycyrrhizin exhibited binding with arginine (ARG-21), glutamine (GLN-63) and arginine (ARG-80) of chain A, A and B, with the hydrogen bond length being 2.005 Å, 2.168 Å and 1.883 Å with nsp7-nsp8 complex of SARS-CoV-2 (6YHU) whereas, Glycyrrhizin with nsp16-nsp10 heterodimer (N7- and 2'O-methyltransferases) in complex with SAM (7C2J) formed hydrogen bond of bond lengths 1.783 Å and 1.788 Å with the methionine (MET-42) and lysine (LYS-76) of chain A, respectively.

Sitosterol with RNA-dependent RNA polymerase (NSP12) in complex with cofactors (6M71) and Clathrin terminal domain complexed with TLPWDLWTT (1UTC) formed hydrogen bond of bond lengths 2.061 Å and 2.012 Å with the asparagine (ASN-100) and methionine (MET-32) of chain B, respectively. Whereas, Piperine with Main Protease (NSP5) (6Y2E) formed hydrogen bond of bond lengths 1.926 Å and 2.16 Å with the lysine (LYS-12) and threonine (THR-304) of chain B, respectively.

The binding affinities of these compounds, along with those of a few previously reported inhibitors such as arbidol (26), hydroxychloroquine (27), ivermectin (28), lopinavir (29), ritonavir (29) and remdesivir (30), are given in supplementary (Table 2). Considering ivermectin as a reference, we note that the inhibition potentials of the isovitexin, glycyrrhizin, sitosterol, and piperine are very encouraging. Ivermectin is an FDA-approved broad spectrum anti-parasitic agent which is currently used for treatment of COVID-19 since it inhibits the replication of SARS-CoV-2.

Table 3- Docking results of selected ligands with different COVID-19 proteins.

		Binding Energy (kcal/mol)								
S.No.	**Extracted compounds**	**6M3M**	**6M71**	**6VWW**	**6W9C**	**6WXD**	**6Y2E**	**6YHU**	**7C2J**	**1UTC**
1.	Eugenol	-5.75	-3.86	-5.56	-4.92	-5.16	-5.01	-4.51	-5.45	-5.02
2.	Eugenyl acetate	-6.09	-4.25	-5.47	-4.37	-4.96	-5.74	-4.92	-5.24	-5.76
3.	Cinnamaldehyde	-5.21	-4.04	-5.49	-4.53	-5.17	-5.16	-4.48	-5.33	-5.25
4.	Allicin	-4.32	-3.67	-4.79	-4.08	-4.08	-4.74	-4.38	-4.56	-4.09
5.	Catechins	-8.02	-5.16	-7.38	-7.48	-7.1	-6.2	-6.46	-7.73	-7.97
6.	Rhaponticin	-7.72	-5.46	-5.44	-6.59	-7.23	-6.24	-5.73	-5.65	-9.45
7.	Isovitexin	-9.37	-6.6	-9.32	-8.24	-9.36	-6.97	-6.53	-6.86	-9.74
8.	Thymoquinone	-5.48	-4.45	-5.67	-4.78	-5.56	-5.61	-5.43	-5.67	-5.84
9.	α -pinene	-5.1	-4.16	-5.21	-4.94	-5.02	-4.96	-5.95	-5.39	-5.41
10.	Swertiamarin	-6.87	-4.79	-6.38	-5.44	-6.23	-6.46	-5.97	-6.12	-6.44
11.	Mangiferin	-6.59	-5.2	-7.02	-5.93	-7.07	-5.93	-4.52	-7.05	-7.04
12.	Glycyrrhizin	-10.9	-6.11	-8.18	-6.67	-7.19	-6.87	-7.93	-8.58	-9.77
13.	Berberine	-7.81	-6.64	-7.14	-6.39	-8.02	-6.84	-7.41	-8.38	-8.4
14.	Sitosterol	-9.25	-7.19	-9.0	-6.95	-5.83	-6.24	-5.91	-7.71	-10.03
15.	Curcumin	-7.82	-6.55	-6.84	-8.0	-8.61	-6.59	-6.44	-7.08	-8.5
16.	Gingerol	-6.42	-4.45	-5.57	-5.43	-5.79	-4.86	-5.1	-5.81	-6.41
17.	Shogaol	-6.94	-4.87	-5.69	-5.63	-6.15	-5.02	-5.03	-5.84	-7.0
18.	Thymol	-5.47	-4.41	-5.06	-4.59	-5.4	-4.75	-5.58	-5.46	-5.83
19.	Piperine	-7.7	-7.01	-6.73	-6.51	-8.06	-7.28	-6.73	-7.83	-8.12
20.	1,8-cineole	-5.43	-4.33	-5.97	-4.74	-5.0	-5.5	-6.1	-5.53	-6.13

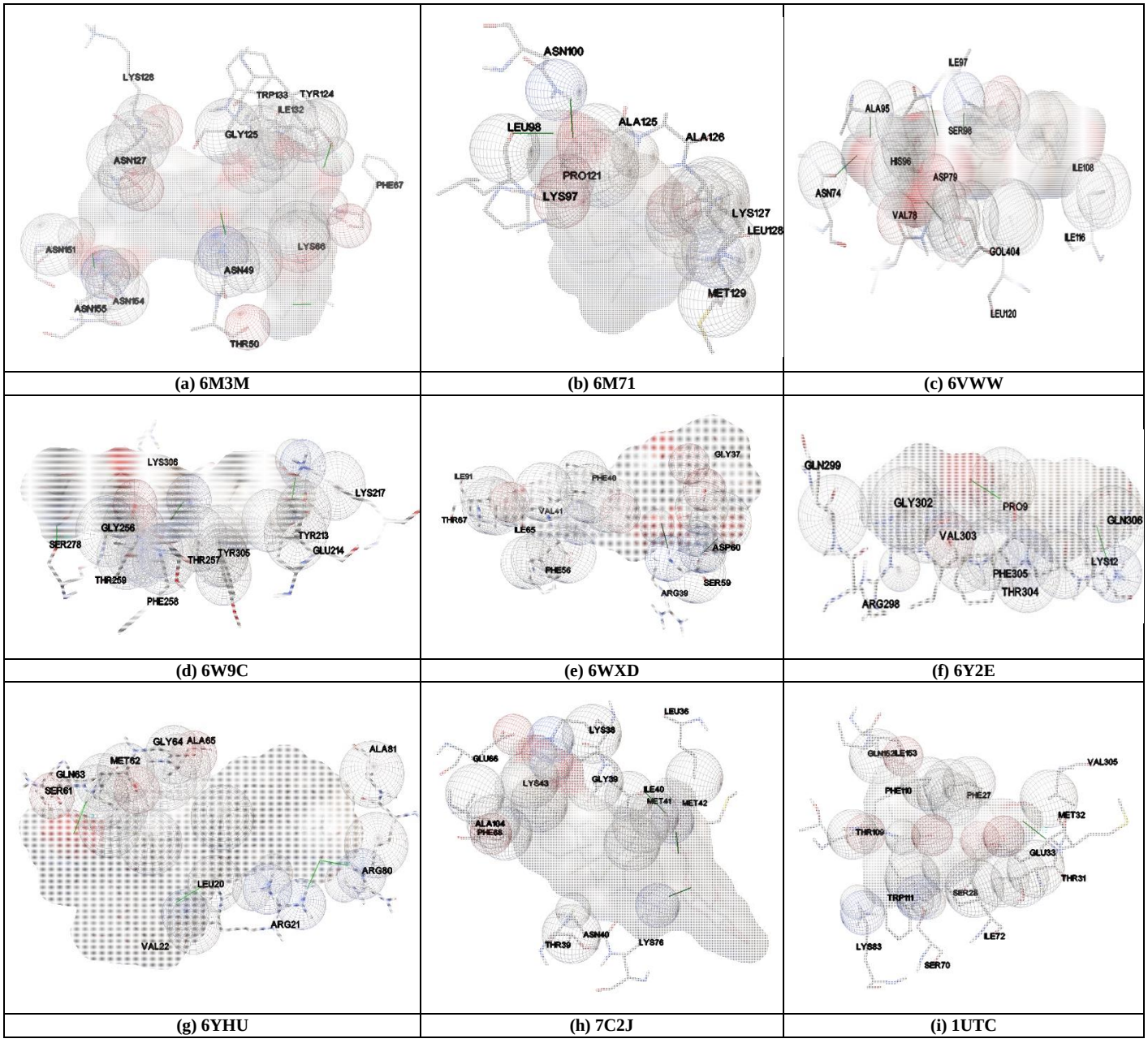

Figure 2. Docking poses of the selected ligands with Covid-19 proteins.

ADME and Toxicity analysis

To predict the pharmacokinetic profile of the potential compounds, an ADME evaluation is required. The physicochemical properties of a compound determine the bioavailability of a compound in the body. The logP represents the lipophilicity of the compound. LogP is the logarithm of the partitioning coefficient between n-octanol and water that has been widely accepted as a descriptor of the lipophilicity of a molecule. LogP values must be in the range of 0-5 (31). It is evident from Table 4 that, except swertiamarin, mangiferin and berberine, all other ligands exhibit positive logP values. One can note that the logP values of most of these compounds lie in the range 2.64-4.95. These values indicate that the compounds can easily diffuse across the cell membranes due to their high organic (lipid) permeability. However, sitosterol, has logP =7.27 (exceeding 5) and therefore possesses high hydrophobicity and poor absorption capacities. On the contrary, allicin, catechins, rhaponticin, isovitexin possess high absorption due to their logP in the range 0.05-1.81.

LogS measures the aqueous solubility, which is crucial physical property related to ADME profile of a compound. Compounds with poor solubility tend to have poor absorption, low stability, and fast clearance. Most of these compounds have logS values higher than -5 (32), except sitosterol, berberine (Table 4), ivermectin, lopinavir and ritonavir (Supplementary Table 13).

In silico ADMET analysis, determining the acceptable properties of pharmacokinetics and pharmacodynamics, is a reliable method. The toxicity risks of selected natural compounds were predicted based on their ADMET profile. In the biological systems, poor pharmacokinetics property and toxicity lead to the failure in drug development. The selected compounds were analyzed for their blood-brain barrier (BBB) penetration, carcinogenicity, subcellular localization, LD50 and category of acute oral toxicity (Table 4) (33).

Depending upon the acute oral toxicity (ADMET prediction profile), compounds are categorized into four groups. Most of the ligands exhibited category III of acute oral toxicity, thus signifying that their LD50 values lie in the range from 500 mg/kg to 5000 mg/kg body weight. Sitosterol exhibited category I of acute oral toxicity, which signifying that their LD50 values less than or equal to 50 mg/kg. Category II contains thymoquinone with LD50 values greater than 50mg/kg but less than 500mg/kg. Category IV consisted of catechins, mangiferin, isovitexin and glycyrrhizin with LD50 values greater than 5000mg/kg.

Table 4. ADME and Toxicity analysis of selected compounds.

		ADME		TOXICITY				
S.NO.	**Extracted compounds**	**LogP**	**LogS**	**Subcellular localization**	**Carcinogenicity**	**Acute Oral Toxicity**	**BBB**	**LD50**
1.	Eugenol	2.66	-2.06	Mitochondria	No	III	+	1.9616
2.	Eugenyl acetate	3.00	-3.14	Mitochondria	No	III	+	2.0606
3.	Cinnamaldehyde	2.00	-2.51	Plasma membrane	No	III	+	1.8598
4.	Allicin	1.16	-1.42	Lysosome	No	III	+	2.5863
5.	Catechins	1.02	-2.65	Mitochondria	No	IV	-	1.8700
6.	Rhaponticin	0.70	-2.86	Mitochondria	No	III	-	2.0773
7.	Isovitexin	0.37	-2.40	Mitochondria	No	IV	-	2.3664
8.	Thymoquinone	2.00	-1.95	Mitochondria	No	II	+	2.6165
9.	α -pinene	3.66	-2.94	Lysosome	No	III	+	1.5348
10.	Swertiamarin	-1.60	-0.95	Mitochondria	No	III	+	2.5442
11.	Mangiferin	-0.09	-1.92	Mitochondria	No	IV	-	2.3664
12.	Glycyrrhizin	2.78	-4.18	Mitochondria	No	IV	-	1.9551
13.	Berberine	-0.18	-6.02	Mitochondria	No	III	+	2.7834
14.	Sitosterol	7.27	-7.35	Lysosome	No	I	+	2.6561
15.	Curcumin	3.62	-4.81	Mitochondria	No	III	+	2.5468
16.	Gingerol	3.45	-3.57	Mitochondria	No	III	+	2.4106
17.	Shogaol	4.95	-4.49	Mitochondria	No	III	+	1.7164
18.	Thymol	3.16	-2.37	Mitochondria	No	III	+	2.2996
19.	Piperine	3.38	-3.28	Mitochondria	No	III	+	2.7129
20.	1,8-cineole	3.36	-3.84	Lysosome	No	III	+	1.8144

CONCLUSIONS

Molecular docking studies are a promising tool for developing more efficient and potential drugs through approaches to ligand-based drug design. In this paper, we have performed an *in- silico* study on the inhibition of proteins associated with COVID-19 by the natural compounds of Indian herbal plants. Based on the binding affinity as well as ADMET analysis, isovitexin, glycyrrhizin, sitosterol, and piperine appear as the most powerful inhibitors among all the compounds considered here. The six drug compounds are already reported to inhibit COVID-19 protease *in vitro*. Due to inherent toxicity and side-effects, however, they are not approved by most of the countries except ivermectin. Herbal plants are alternative method towards the development of herbal medicines having no apparent side-effects.

CONFLICT OF INTEREST

All authors declare no conflict of interest.

ACKNOWLEDGEMENT

Authors are thankful to Director of MNNIT & Department of Biotechnology MNNIT Allahabad, Prayagraj, India.

REFERENCES

1. World Health Organization (WHO). Novel Coronavirus (2019-nCoV) Situation Report – 52. Data as reported by 12 March 2020. Available from https://www.who.int/docs/default-source/coronaviruse/20200312-sitrep-52-covid-19.pdf?sfvrsn=e2bfc9c0_2 Accessed on 12 March 2020.
2. N. Chen, M. Zhou, X. Dong, J. Qu, F. Gong, Y. Han, et al. Epidemiological and clinical characteristics of 99 cases of 2019 novel coronavirus pneumonia in Wuhan, China: a descriptive study. Lancet. 395, 507–13, (2020).
3. J. Lan, J. Ge, J. Yu, S. Shan, H. Zhou, et al. Structure of the SARS-CoV-2 spike receptor-binding domain bound to the ACE2 receptor. Nature. 581, 215–220, (2020).
4. H. Hofmann, S. Pohlmann, Cellular entry of the SARS coronavirus. Trends Microbiol. 12, 466–472, (2004)
5. H. Vennema, G.J. Godeke, J.W. Rossen, W.F. Voorhout, M.C. Horzinek, et al. Nucleocapsid-independent assembly of coronavirus-like particles by co-expression of viral envelope protein genes. EMBO J. 15, 2020–2028, (1996)
6. Y.L. Siu, K.T. Teoh, J. Lo, C.M. Chan, F. Kien, et al. The M, E, and N structural proteins of the severe acute respiratory syndrome coronavirus are required for efficient assembly, trafficking, and release of virus-like particles. J Virol. 82, 11318–11330, (2008)
7. Y. Gao, L. Yan, Y. Huang, F. Liu, Y. Zhao, et al. Structure of the RNA-dependent RNA polymerase from COVID-19 virus. Science. 368, 779–782, (2020)
8. R, Solecki, I.V. Shanidar, a Neanderthal flower burial in Northern Iraq. Science. 190, 880-1, (1975)
9. B.A. Rasool Hassan, Medicinal plants (importance and uses). Pharmaceut Anal Acta. 3, 139, (2012)
10. G. Samuelsson, Drugs of Natural Origin: A Textbook of Pharma¬cognosy, 5th Swedish Pharmaceutical Press, Stockholm. Swedish Phar¬maceutical Press, Stockholm. J Nat Prod, 68 (4), 631, (2004)
11. J. Azmir, I.S.M. Zaidul, M.M. Rahman, K.M. Sharif, A. Mohamed, F. Sahena, M.H.A. Jahurul, K. Ghafoor, N.A.N. Norulaini, A.K.M. Omar. Techniques for extraction of bioactive compounds from plant materials: A review. Journal of Food Engineering. 117, 426-436, (2013)
12. P.S. Masters, L.S. Sturman, Background Paper Functions of the Coronavirus Nucleocapsid Protein. In Coronaviruses and Their Diseases (Cavanagh, D. and Brown, T.D.K.eds), Springer US, Boston, MA, (1990)
13. L. Subissi, C.C. Posthuma, J.C. Collet, Zevenhoven-Dobbe, A.E. Gorbalenya, E. Decroly, et al, One severe acute respiratory syndrome coronavirus protein complex integrates processive RNA polymerase and exonuclease activities. Proc. Natl Acad. Sci U.S.A.111, E3900 (2014)
14. Z.J. Miknis, E.F. Donaldson, T.C. Umland, R.A. Rimmer, R.S. Baric, L.W. Schultz, Severe acute respiratory syndrome coronavirus nsp9 dimerization is essential for efficient viral growth. J. Virol. 83, 3007–3018, (2009)
15. R. Ulferts, J. Ziebuhr, Nidovirus ribonucleases: structures and functions in viral replication. RNA Biol. 8, 295–304, (2011)
16. W. Rut, Z. Lv, M. Zmudzinski, S. Patchett, D. Nayak, S.J. Snipas, et al, Activity profiling and crystal structures of inhibitor-bound SARS-CoV-2 papain-like protease: A framework for anti -COVID-19 drug design. Science Advances 6, eabd4596, (2020)

17. T. Muramatsu, Y.T. Kim, W. Nishii, T. Terada, M. Shirouzu, S. Yokoyama, Autoprocessing mechanism of severe acute respiratory syndrome coronavirus 3C-like protease (SARS-CoV 3CLpro) from its polyproteins FEBS J. 280, 2002–2013, (2013)
18. P. Krafcikova, J. Silhan, R. Nencka, E. Boura, Structural analysis of the SARS-CoV-2 methyltransferase complex involved in RNA cap creation bound to sinefungin. Nat. Commun. 11, 3717, (2020)
19. S.D. Conner, S.L. Schmid, Regulated portals of entry into the cell. Nature, 422, 37–44 (2003)
20. S. Srivastava & A. Pandey, Computational screening of anticancer drugs targeting miRNA155 synthesis in breast cancer. Indian Journal of Biochemistry & Biophysics, 57, 389-394, (2020)
21. I. Singha, S. Saxena, S. Gautam, A. Saha & S.K. Das, Grape extract protect against ionizing radiation-induced DNA damage. Indian J Biochem Biophys, 57, 219, (2020)
22. A. Ganeshpurkar & A. Saluja, In silico interaction of rutin with some immunomodulatory targets: a docking analysis. Indian J Biochem Biophys, 55, 88, (2018)
23. I.V. Tetko & V.Y. Tanchuk, Application of associative neural networks for prediction of lipophilicity in ALOGPS 2.1 program. J Chem Inf Comput Sci, 42, 1136, (2002)
24. F. Cheng, W. Li, Y. Zhou, J. Shen, Z. Wu, G. Liu, P.W. Lee & Y. Tang, admetSAR: a comprehensive source and free tool for assessment of chemical ADMET properties. J Chem Inf Model, 52, 3099, (2012)
25. A. Basu, A. Sarkar, U. Maulik & P. Basak, Three-dimensional structure prediction and ligand-protein interaction study of expansin protein ATEXPA23 from Arabidopsis thaliana L. Indian J Biochem Biophys, 56, 20, (2019)
26. J. Blaising, S.J. Polyak, E.I. Pécheur, Arbidol as a broad-spectrum antiviral: An update. Antiviral Res. 107, 84–94, (2014)
27. P. Gautret, J.C. Lagier, P. Parola, V.T. Hoang, L. Meddeb, et al, Hydroxychloroquine and azithromycin as a treatment of COVID-19: results of an open-label non-randomized clinical trial. Int J Antimicrob Agents – In Press 17 March 2020.
28. L. Caly, J.D. Druce, M.G. Catton, D.A. Jans, K.M. Wagstaff, The FDA-approved drug ivermectin inhibits the replication of SARS-CoV-2 in Vitro. Antiviral Research, 178, 104787, (2020)
29. ClinicalTrials.gov [Internet]. Bethesda (MD): National Library of Medicine (US). Mar 12 – Identifier NCT04252885, The efficacy of lopinavir plus ritonavir and arbidol against novel coronavirus infection (ELACOI), (2020)
30. ClinicalTrials.gov [Internet]. Bethesda (MD): National Library of Medicine (US). Mar 12 – Identifier NCT04257656, Severe2019-nCoV Remdesivir RCT, (2020)
31. S.K. Bhal, LogP—making sense of the value. Advanced Chemistry Development, (Toronto, ON, Canada), 1, (2007)
32. W.L. Jorgensen, & E.M. Duffy, Prediction of drug solubility from Monte Carlo simulations. Bioor. Med. Chem. Lett. 10, 1155-1158, (2000)
33. F. Cheng, W. Li, Y. Zhou, J. Shen, Z. Wu, G. Liu, P.W. Lee & Y. Tang, admetSAR: a comprehensive source and free tool for assessment of chemical ADMET properties. J Chem Inf Model, 52, 3099, (2012)